Structural Eng./Earthquake Eng. Vol. 11, No. 1, 45s—52s, April 1994
Japan Society of Civil Engineers (J. Struct. Mech. Earthquake Eng. No. 489/I—27)

FATIGUE CRACK GROWTH RATE MEASUREMENT OF STRUCTURAL STEEL UNDER OVERLOAD CONDITIONS

Xiaohua CHENG*, Yuji OKUHARA**,
Kentaro YAMADA*** and Akimasa KONDO****

Fatigue crack growth behavior under single-peak overloads is investigated for structural steel JIS SM520B. Fatigue test is carried out on seven center prenotched specimens. Three parameters, i.e. overload ratio, overload application stage and stress ratio are introduced to investigate the retardation effect. It is verified that fatigue crack growth rate is retarded after overloading and then gradually recovers to the normal. It is also observed that the retardation effect is intensified when the overload ratio and the stress range between overload stress and the following minimum stress increase. From the test results the crack length increment in which retardation occurs is compared with Irwin's and Dugdale's plastic zone sizes.

Key Words : *Fatigue, Crack growth rate, Overload, Retardation, Plastic zone size*

1. INTRODUCTION

Miner's rule or equivalent stress range concept is normally used in fatigue life estimation of structural members subjected to variable amplitude loading. The method is simple and widely used in various fatigue design codes. In order to keep its simplicity, the method does not consider the load interaction effect of various load sequences, for example, high-low, low-high, low-high-low or high-low-high and random sequence[1]. When a structure is subjected to several higher stress cycles among a large number of lower stresses, for example in case of highway bridges, the interaction effect of high-low load sequence may occur[2]. In order to develop more accurate computational model for fatigue crack growth under variable amplitude loading, the interaction effect is to be re-examined.

A single overload or multiple-overload reduces fatigue crack growth rate significantly at the lower stress range level following the overloads[2),3)]. Some of the observations have been reported elsewhere[4),5),6)]. A large plastic zone and residual plastic deformation formed near crack tip due to overloading and unloading enhance crack closure in the wake of an advancing crack tip[7)]. It causes a retardation effect on crack growth. The parameters, such as overload level, overload application stage, stress range, stress ratio, the number of overload cycles, plate thickness and material strength may affect the retardation effect[6),8)].

* Graduate Student, Dept. of Civil Eng., Nagoya Univ., Nagoya, 464-01, JAPAN
** Graduate Student, Dept. of Civil Eng., Nagoya Univ.
*** Member of JSCE, Ph. D., Professor, Dept. of Civil Eng., Nagoya Univ.
**** Member of JSCE, Dr. Eng., Associate Professor, Dept. of Civil Eng., Meijo Univ., Nagoya, 468, JAPAN

In the present study, fatigue crack growth rate measurement is carried out on center prenotched specimens of structural steel SM520B under constant amplitude (CA) loading and single-peak overload conditions. Three parameters are chosen to investigate retardation effect: (1) overload ratio, $R_{OL} = \sigma_{OL}/\sigma_{max}$, which expresses overload level; (2) overload application stage during crack growth, expressed by stress intensity factor range, ΔK; and (3) stress ratio, $R = \sigma_{min}/\sigma_{max}$, which is the stress ratio of CA loading following overloads. The crack length increment in which retardation occurs is compared with Irwin's plastic zone size and Dugdale's plastic zone size.

2. EXPERIMENTS

(1) Test specimens and load patterns

Fatigue crack growth rates were measured on center prenotched test specimens of structural steel SM520B (**Table 1**), as shown in **Fig.1**. The prenotch was manufactured by electrodischarge machining. Both surfaces of specimen were mirror-polished for easy observation of fatigue crack by microscopes. Constant amplitude loading and single-peak overloading were applied to specimens. The typical load pattern is shown in **Fig.2**. Seven specimens were tested under various stress levels R and overload levels R_{OL}, as shown in **Table 2**.

(2) Test procedure

The test was carried out in an ambient environment. The load was applied parallel to the rolling direction of the material by a servo type fatigue testing machine with a capacity of 245 KN. The loading frequency was 8~10 Hz. Overloads were applied at 0.05 Hz. Crack growth was observed optically with two traveling microscopes of 25x magnification on each side of the specimen. The test

Table 1 Mechanical properties and chemical composition of JIS SM520B steel

Mechanical properties (MPa)			Chemical composition (%)								
Yield strength σ_s	Tensile strength σ_u	Elongation (%)	C	Si	Mn	P	S	Cu	Ni	Cr	V	Ceq
401.8	539	24	0.16	0.34	1.32	0.014	0.006	-	-	-	0.04	0.40

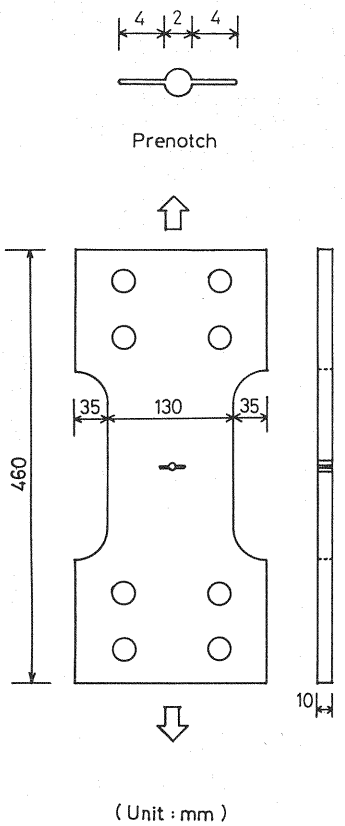

Figure 1 Center prenotched specimen

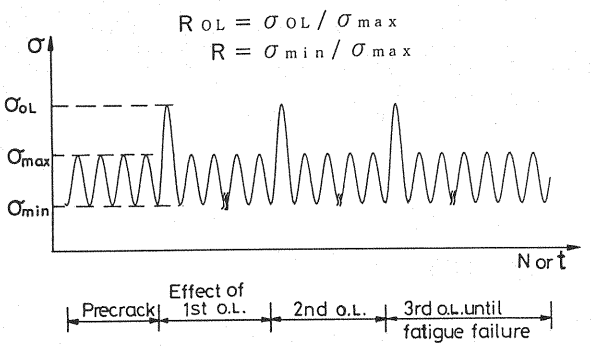

Figure 2 Single-peak overload pattern used in the test

Table 2 Specimens for single overload test

Spec. No.	$\Delta\sigma$ (MPa)	σ_{max} (MPa)	σ_{min} (MPa)	R	R_{OL}	σ_{OL} (MPa)
A-CA	70	90	20	0.22	-	-
A-OLH	70	90	20	0.22	2.0	180
A-OLM	70	90	20	0.22	1.7	153
A-OLL	70	90	20	0.22	1.4	126
B-CA	70	130	60	0.46	-	-
B-OLL	70	130	60	0.46	1.4	182
B-OLLL	70	130	60	0.46	1.2	156

set-up is shown in **Fig.3**. The definition of fatigue crack length is shown in **Fig.4**. Precracks of about 3~4 mm from the prenotches were introduced before crack growth measurement was started. Constant amplitude fatigue test was carried out on two specimens starting at a crack growth rate level of about da/dN=10^{-8} m/cycle. According to the previous test data[9),10)], the corresponding stress intensity factor range is $\Delta K \approx 11$ MPa$\sqrt{m}$. For a crack size of $a \approx 8$ mm, the corresponding stress range is about 70 MPa. Tests were carried out at two stress ratios of R=0.22 and 0.46. Five specimens were tested under overload conditions. For each specimen overloads were applied three times at the different stages. Four overload ratio R_{OL} were selected as 2.0, 1.7, 1.4 and 1.2.

3. FATIGUE CRACK GROWTH RATES

(1) Results of crack growth measurement

Fatigue crack growth rates are measured in a range of ΔK from about 10 to 30 MPa$\sqrt{m}$ under CA and overload conditions. The relation between crack length a and the number of cycles N of each specimen is shown in **Figs.5** and **6**. Stable change in crack growth rates is observed under CA loading, while under overload conditions the crack growth deviates from that of CA loading after overloads are applied. For A-Series specimens, crack growth rate (a)

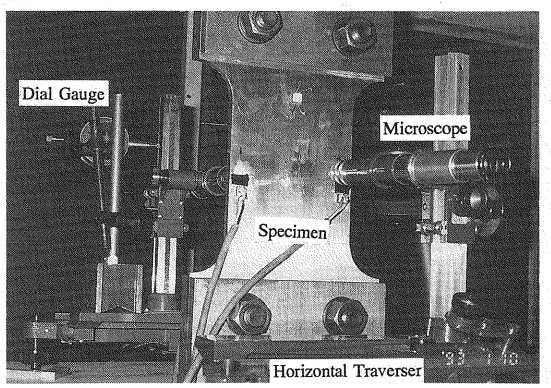

Figure 3 Test set-up for fatigue crack growth measurement

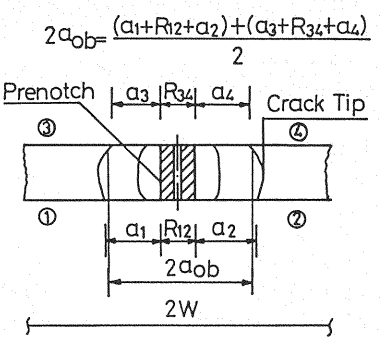

Figure 4 Schematic drawing of profile of crack front and definition of crack length

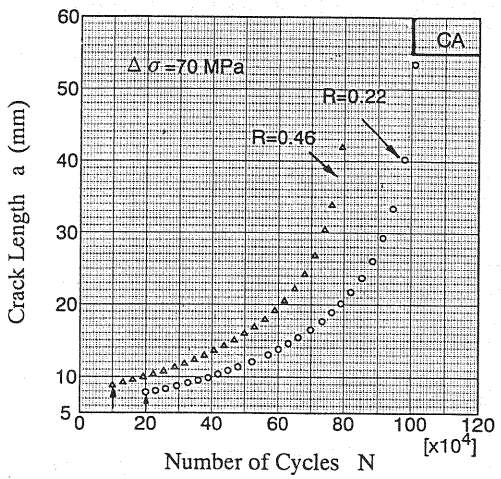

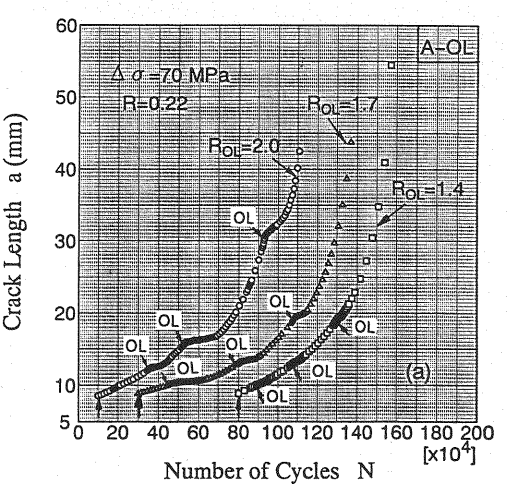

Figure 5 Fatigue crack growth under CA loading

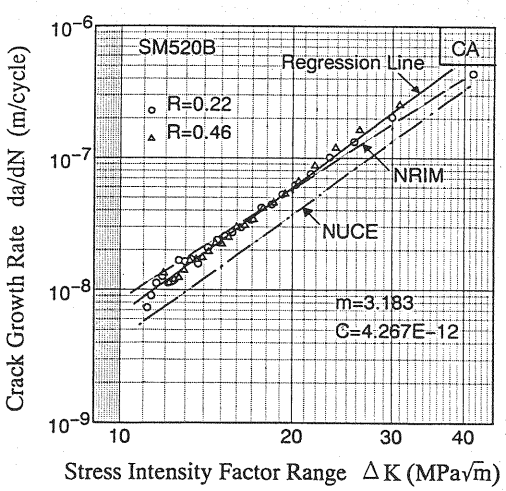

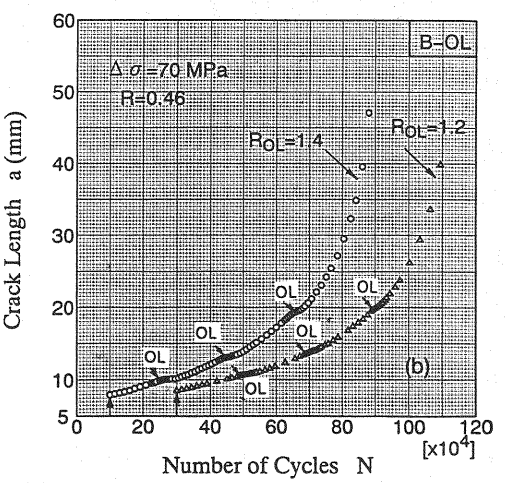

Figure 7 Fatigue crack growth rates under CA loading

Figure 6 Fatigue crack growth under overload conditions

firstly increases slightly, (b) decreases significantly for a certain period, and then (c) recovers to the same crack growth rate as that before overloading. For B-Series specimens, no increase in crack growth rate after overload is observed. The delayed life due to overload decreases as fatigue crack grows, i.e. as the stress intensity factor range ΔK increases. Also, the delayed life becomes shorter when overload ratio R_{OL} is lower (see **Figs.6(a)** and **6(b)**). From the observation of fatigue fracture surface, the crack length at inner crack tip is longer than the crack length at the plate surface observed by the microscope. Based on the measurement of the crack tips due to overloads, the actual crack tip is proposed by the empirical equation as follows:

$$a \approx 1.01a_{ob} + 0.50 \quad (mm) \quad \cdots\cdots (1)$$

where a is the crack length at inner crack tip and a_{ob} is the observed crack length at the specimen surfaces. In present experimental study, the crack length is taken as a, as shown in Eq.(1).

(2) Fatigue crack growth rates

The crack growth rates under CA loading are shown in **Fig.7** along with the previous test results[9),10)]. The two fatigue crack growth rate measurements under stress ratios R=0.22 and R=0.46 show almost the same fatigue crack growth rates, and are almost identical to the data obtained by the National Research Institute for Metals (NRIM)[9)]. They are slightly higher compared with the previous test data (NUCE) obtained on the compact specimens[10)]. The empirical equation of da/dN can be expressed as:

$$\frac{da}{dN} = C(\Delta K)^m \quad \cdots\cdots (2)$$

where the material constants m = 3.183 and C = 4.267×10^{-12} are determined by the least square method.

The fatigue crack growth rates under overload conditions are shown in **Fig.8**. The test data under overload conditions are smoothened by B-spline function, as shown by the dotted lines. The solid line is the crack growth rates under CA loading. It is noted that crack growth rates under overload deviate from those of CA loading after overload application. The crack growth rates of A-Series specimens under overload conditions firstly increase a little, then rapidly decrease to the minimum value, and finally gradually recover to that of CA loading. The higher overload ratio causes the deeper valley of da/dN after overload application which means more intensified retardation effect. At lower ΔK level, crack growth retardation is more pronounced. Therefore, compared with the crack growth rates of CA loading, the crack growth rates are retarded after overload application.

Moreover, the test results show that at the same overload ratio R_{OL}, for example, specimens A-OLL and B-OLL, more intensified retardation effect occurs at higher stress ratio R due to the much higher overload level. When approximately same overload σ_{OL} is applied, for example, σ_{OL} = 180 and 182 MPa for the specimens A-OLH and B-OLL, respectively, more intensified retardation effect is observed at lower stress ratio R. The same is observed for A-OLM and B-OLLL, where σ_{OL} = 153 and 156 MPa, respectively. Therefore, retardation effect is affected by overload ratio, overload peak value, stress ratio, and consequently the stress range between σ_{OL} and the minimum stress σ_{min}.

4. COMPARISON WITH PLASTIC ZONE SIZE

(1) Crack growth rate versus crack length

The crack growth rates are plotted against crack length in **Fig.9** for specimen A-OLM. The circular symbols show the test data and the solid line is the smoothened curve of the test data. In this stage, we can define retardation affected zone Δa_{OL}. Δa_{OL} is the crack length increment from the overload application to the end of the retardation effect. In the present experiment, the point where retardation effect ends is determined by the test data point where crack growth rate on the smoothened curve becomes stable and close to the crack growth rates of CA loading. Δa_{OL} increases as crack length a increases, *i.e.* as ΔK increases. The point of the minimum crack growth rate after overload is also determined by the smoothened curve.

(2) Plastic zone size

The residual plastic deformation remaining in the wake of an advancing crack tip causes crack closure[7)]. The plastic zone size due to overload at crack tip plays an important role in determining the retardation effect. Here we compare the length Δa_{OL}, with Irwin's plastic zone size[3)] and Dugdale's plastic zone size[3),11)] under overload σ_{OL}. In case of finite plate width, they can be expressed as follows:

Irwin's plastic zone size, ρ_{Irw} :

$$\rho_{Irw} = \frac{1}{\pi}\left(\frac{K_{OL}}{\sigma_{ys}}\right)^2 \quad \cdots\cdots (3)$$

Dugdale's plastic zone size, ρ_{Dug} :

$$\rho_{Dug} = a\left\{\frac{2W}{\pi a}\sin^{-1}\left[\sin\left(\frac{\pi a}{2W}\right)\sec\left(\frac{\pi\sigma_{OL}}{2\sigma_{ys}}\right)\right] - 1\right\} \quad \cdots\cdots (4)$$

where the plastic zone size is along the direction of crack growth, W is the half plate width of specimen, K_{OL} is the stress intensity factor under overload with

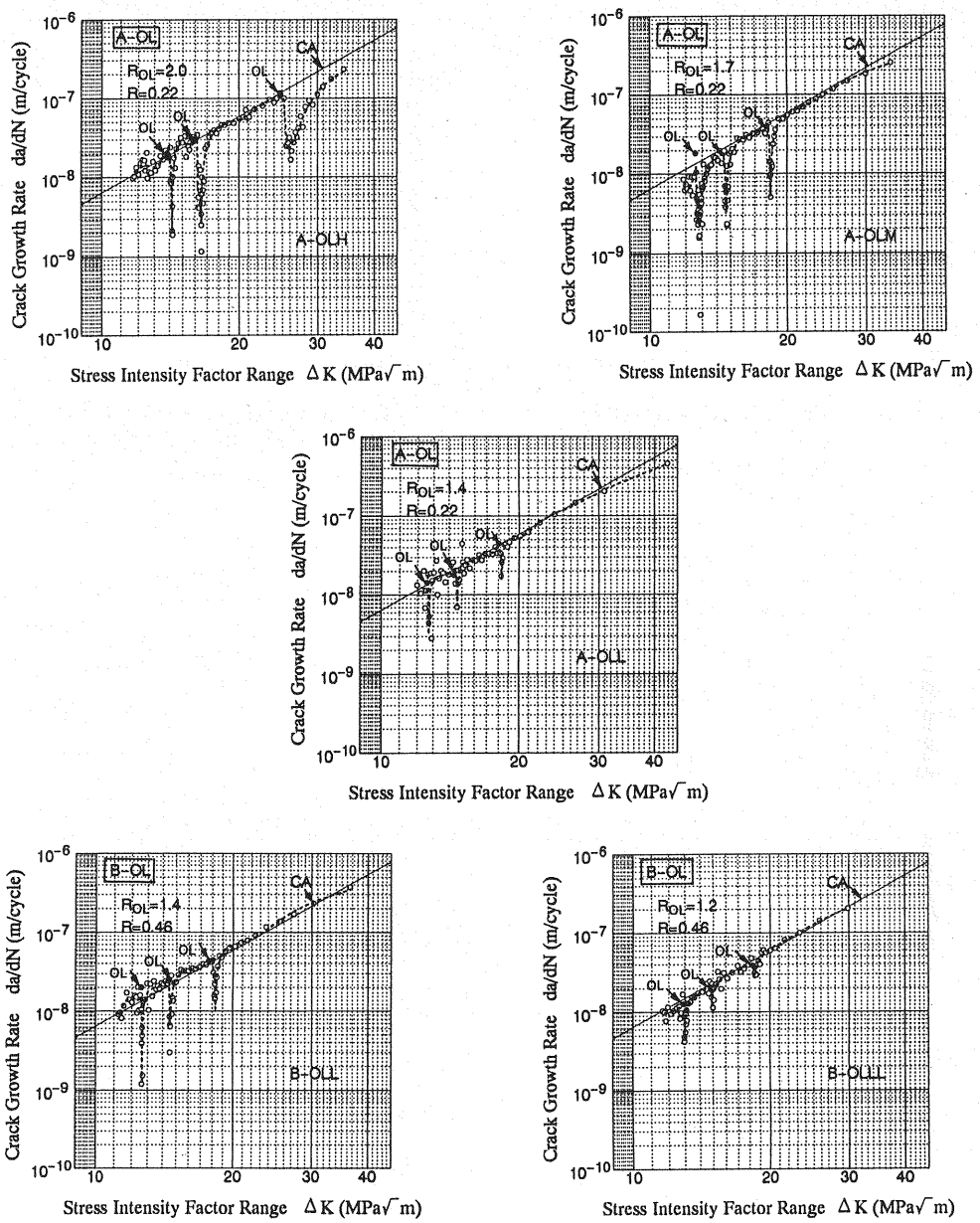

Figure 8 Fatigue crack growth rates under overload conditions

the finite plate width correction and σ_{ys} is the equivalent yield stress corresponding to the plane stress state or the plane strain state. The constraint factor α which is defined as $\alpha = \sigma_{ys}/\sigma_s$ expresses the constraint effect in the direction of plate thickness on plastic deformation at crack tip. σ_s is the yield strength of material. α=1 corresponds to the plane stress state and α=1.68 corresponds to the plane strain state at crack tip[12]. Plane strain condition yields smaller plastic zone size at crack tip.

The models of Irwin's plastic zone size and Dugdale's plastic zone size are both based on the assumptions of elastic-perfectly plastic material and small plastic zone size compared with the crack size. Based on the stress analysis of cracked body and von Mises yield criterion, ρ_{Irw} in Eq.(3) can be obtained by considering equilibrium of stresses after plastic relaxation[3]. In Dugdale's plastic zone model, it is assumed that the plastic deformation is concentrated in a localized strip in front of the crack, forming a fic-

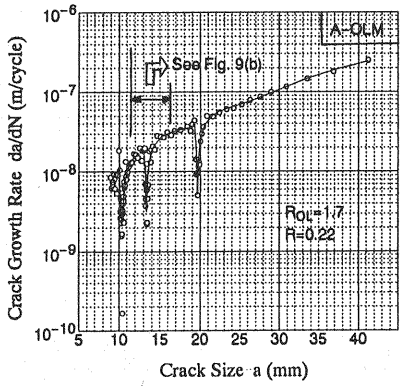

(a) da/dN measurement of specimen A-OLM

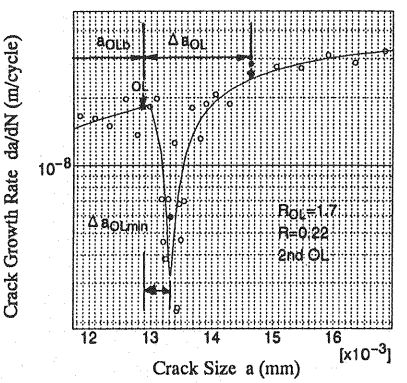

(b) Close up view of crack length increment after overloading

Figure 9 Fatigue crack growth rate retardation after overloading

Table 3 Plastic zone size and crack length increment

Spec.	O.L.	a_{OLb} (mm)	K_{OL} ($MPa\sqrt{m}$)	Δa_{OL} (mm)	$\alpha = 1.0$		$\alpha = 1.68$		Δa_{OLmin} (mm)	$\frac{\Delta a_{OLmin}}{\Delta a_{OL}}$
					$\frac{\Delta a_{OL}}{\rho_{Irw}}$	$\frac{\Delta a_{OL}}{\rho_{Dug}}$	$\frac{\Delta a_{OL}}{\rho_{Irw}}$	$\frac{\Delta a_{OL}}{\rho_{Dug}}$		
A-OLH	1st†	12.87	37.06	1.50	0.55	0.36	1.56	1.19	0.32	1/4.69
	2nd	16.38	42.46	3.15	0.89	0.57	2.50	1.91	0.67	1/4.70
	3rd	31.17	65.79	8.15	0.96	0.55	2.70	2.12	1.50	1/5.43
A-OLM	1st	10.64	28.42	1.49	0.94	0.65	2.66	2.04	0.38	1/3.92
	2nd	13.66	32.55	1.84	0.88	0.61	2.49	1.94	0.39	1/4.72
	3rd	19.79	40.40	2.90	0.90	0.62	2.54	2.00	0.58	1/5.00
A-OLL	1st	10.63	23.39	0.77	0.71	0.52	2.03	1.60	0.17	1/4.53
	2nd	13.66	26.80	0.93	0.65	0.48	1.86	1.48	0.25	1/3.72
	3rd	19.81	33.32	1.68	0.77	0.57	2.18	1.75	0.31	1/5.42
B-OLL	1st	10.00	33.75	0.98	0.44	0.28	1.24	0.93	0.10	1/9.80
	2nd	13.00	38.68	1.54	0.52	0.33	1.47	1.12	0.08	1/19.25
	3rd	19.76	48.03	3.13	0.69	0.43	1.94	1.49	0.42	1/7.45
B-OLL	1st	11.21	29.80	0.71	0.41	0.28	1.15	0.89	0.05	1/14.2
	2nd	14.31	34.06	0.85	0.37	0.26	1.05	0.85	0.12	1/7.08
	3rd	20.38	41.97	2.24	0.65	0.44	1.82	1.44	0.31	1/7.23

* a_{OLb} is the crack length just before overload application.
** $K_{OL} = \sigma_{OL}\sqrt{\pi a_{OLb}}\,(1 - 0.025(a_{OLb}/W)^2 + 0.06(a_{OLb}/W)^4)\sqrt{sec(\pi a_{OLb}/2W)}$
*** † Data on this line are not used in comparison.

titious crack which is surrounded by an elastic stress field[3),11)]. ρ_{Dug} in Eq.(4) is derived on the basis of assumption of non-singularity at fictitious crack tip. For an infinite plate width and a load of $\sigma_{OL} < 0.6\sigma_s$, ρ_{Dug} becomes approximately:

$$\rho_{Dug} = \frac{\pi}{8}\left(\frac{K_{OL}}{\sigma_{ys}}\right)^2 \quad \cdots\cdots (5)$$

Therefore, ρ_{Dug} is a little larger than ρ_{Irw} (ρ_{Dug}=1.23ρ_{Irw}) in case of infinite plate width. For finite plate width, ρ_{Dug} is even larger than ρ_{Irw}, and it depends on the crack length. Irwin's plastic zone size is generally used due to its simple expression, while Dugdale's plastic zone size is normally used due to the simple assumption of plastic deformation surrounding the crack.

Supposing that σ_s=401.8 MPa for SM520B steel and the constraint factors α=1.0 and 1.68, the comparison between Δa_{OL} and plastic zone size ρ based on Eqs.(3) and (4) are shown in **Table 3** and **Fig.10**.

(3) Results of comparison

It is noted that even though Δa_{OL} increases as ΔK increases, the ratio $\Delta a_{OL}/\rho$ is almost constant. The value of $\Delta a_{OL}/\rho$ does not change appreciably with

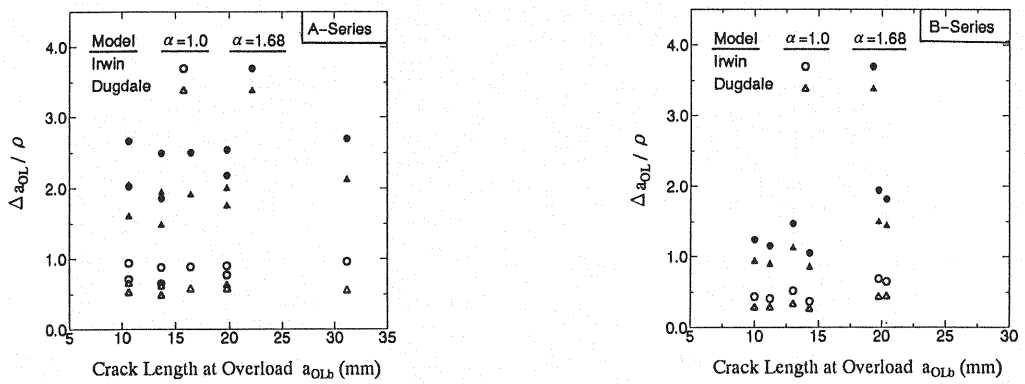

Figure 10 Comparison of Δa_{OL} and plastic zone size

changing overload ratio R_{OL} for a certain model of plastic zone size. For A-Series specimens (R=0.22), Δa_{OL} is less than both Irwin's plastic zone size ρ_{Irw} and Dugdale's plastic zone size ρ_{Dug} when α=1.0, that is, $\Delta a_{OL}/\rho$ is between 0.5 and 1.0. However if α = 1.68, $\Delta a_{OL}/\rho$ is between 1.5 and 2.7 which means Δa_{OL} is larger than both ρ_{Irw} and ρ_{Dug}. For B-Series specimens (R=0.46), $\Delta a_{OL}/\rho$ is less than that of A-Series specimens. It indicates that with the increasing value of stress ratio R, the value of $\Delta a_{OL}/\rho$ decreases. The crack tip blunting under overload at the higher stress level and consequently the less crack closure upon unloading may contribute to the less intensified retardation. The ratio of $\Delta a_{OL}/\rho$ normally implies when or where the retardation effect diminishes after overload application. The experimental result of Matsuoka *et al.* gives the value of this ratio equal to 1.5 at α=1.0 for HT80 steel[13].

Δa_{OLmin} as shown in **Fig.9(b)** is the crack length increment, which is from overload application to the minimum of crack growth rate, is also compared with Δa_{OL}. It is noted that for A-Series specimens Δa_{OLmin} is approximately equal to one-fourth or one-fifth of Δa_{OL}. For B-Series specimens, $\Delta a_{OLmin}/\Delta a_{OL}$ is less than that of A-Series, which means that with the increase of stress ratio the crack growth rate reaches its minimum value relatively faster after the overload application.

5. SUMMARY

Fatigue crack growth rates are measured on center prenotched specimens of JIS SM520B steel under CA and overload conditions. Crack growth retardation effect is investigated for three parameters, i.e. overload ratio, overload application stage and stress ratio. The crack length where retardation effect is observed is compared with Irwin's plastic zone size and Dugdale's plastic zone size. The followings summarize the results:

1. Crack growth rates under CA loading can be expressed by Paris' empirical equation for JIS SM520B steel, where m=3.183 and C=4.267 $\times 10^{-12}$. It agrees well with the previous test results.

2. The crack growth retardation behavior is observed in structural steel after overloads. The higher the overload ratio is, the more intensified the retardation effect is. The lower the stress intensity factor range at overload application is, the more intensified the retardation effect is.

3. Retardation effect is affected by overload ratio, overload peak value, stress ratio, and consequently the stress range between overload peak and the minimum stress.

4. The crack length increment Δa_{OL} over which retardation effect is observed increases as ΔK increases. But the ratio $\Delta a_{OL}/\rho$ remains almost constant for a particular loading condition. With the increasing value of stress ratio R, $\Delta a_{OL}/\rho$ decreases. Furthermore, the value of the ratio does not change appreciably with changing overload ratio R_{OL}.

ACKNOWLEDGEMENTS

This experimental study is supported by Nagoya Expressway Public Corporation. The test specimens are fabricated by Topy Industries, Ltd. The authors are grateful for their support and help.

REFERENCES

1) Rolfe, S.T. and Barsom, J.M. : Fracture and Fatigue Control in Structures - Application of fracture mechanics, Prentice-Hall Inc., Englewood Cliffs, New Jersey, 1977.

2) Hertzberg, R.W. : Deformation and Fracture Mechanics of Engineering Materials, John Wiley and Sons Inc., pp.496~498, 1976.

3) Meguid, S.A. : Engineering Fracture Mechanics, Elsevier Applied Science, 1989.

4) Mitsugi, Y., Ohno, T. and Yamada, K. : Fatigue behavior of preoverloaded notched and gusseted specimens, *Proc. of JSCE, Structural Eng./Earthquake Eng.*, No. 368/I-5, pp.293~300, April, 1986 (in Japanese).

5) Yamada, K. and Cheng, X. : Fatigue life analysis on welded joints under various spectrum loadings, *Journal of Structural Engineering, JSCE*, Vol. 39A, pp.947~957, March, 1993.

6) Himmelein, M.K. and Hillberry, B.M. : Effect of stress ratio and overload ratio on fatigue crack delay and arrest behavior due to single peak overloads, *Mechanics of Crack Growth*, ASTM STP 590, pp.321~330, Feb., 1976.

7) Elber, W. : The significance of fatigue crack closure, *Damage Tolerance in Aircraft Structures*, ASTM STP 486, pp.230~242, 1971.

8) Nishitani, H. : Theory of Fatigue Strength, Ohmu, p.254, 1985 (in Japanese).

9) National Research Institute for Metals : Fatigue crack propagation properties in arc-welded butt-joints of high strength steels for welded structure, *NRIM Fatigue Data Sheet Technical Document*, No. 3, p.37, 1984 (in Japanese).

10) Yamada, K. : Fatigue crack growth rates of structural steels under constant and variable amplitude block loading, *Proc. of JSCE, Structural Eng./Earthquake Eng.*, Vol. 2, No. 2, pp.25~33, Oct., 1985.

11) Newman, J.C. Jr. : A crack-closure model for predicting fatigue crack growth under aircraft spectrum loading, *Methods and Models for Predicting Fatigue Crack Growth under Random Loading*, ASTM STP 748, pp.53~84, Oct., 1981.

12) Gao, Q.: Engineering Fracture Mechanics, Chongqing University, China, p.53, 1986 (in Chinese).

13) Matsuoka, S., Tanaka, K. and Kawahara, M. : The retardation phenomenon of fatigue crack growth in HT80 steel, *Engineering Fracture Mechanics*, Vol. 8, pp.507~523, 1976.

(Received August 2, 1993)